ResearchGate

See discussions, stats, and author profiles for this publication at: https://www.researchgate.net/publication/20823589

# Small-angle neutron scattering study of the structure of protein / detergent complexes

**ARTICLE** *in* BIOPOLYMERS · FEBRUARY 1990

Impact Factor: 2.39 · DOI: 10.1002/bip.360290206 · Source: PubMed

CITATIONS
126

READS
47

**4 AUTHORS**, INCLUDING:

Sow-Hsin Chen
Massachusetts Institute of Technology
**469** PUBLICATIONS **15,574** CITATIONS
SEE PROFILE

José Teixeira
French National Centre for Scientific Research
**206** PUBLICATIONS **5,235** CITATIONS
SEE PROFILE

Available from: José Teixeira
Retrieved on: 24 January 2016

# Small-Angle Neutron Scattering Study of the Structure of Protein / Detergent Complexes

X. H. GUO, N. M. ZHAO,* S. H. CHEN,† and J. TEIXEIRA**

Department of Nuclear Engineering and Biotechnology Process Engineering Center, Massachusetts Institute of Technology, Cambridge, Massachusetts 02139;
**Laboratoire Leon Brillouin, C.E.A. Saclay, 91191 Gif-Sur-Yuette Cedex, France

SYNOPSIS

Small-angle neutron scattering (SANS) was used to study the structure of protein/sodium dodecylsulfate complexes. Two water soluble proteins, bovine serum albumin (BSA) and ovalbumin (OVA), were used. The protein concentration was kept constant at 1 wt %, and protein/detergent wt ratio varied between 1/1, 1/1.5, 1/2 and 1/3. Absolute intensities of SANS distributions were analyzed by a fractal model. Analyses of large $Q$ portions of SANS distributions established that sodium dodecylsulfate (SDS) molecules bound to a protein/SDS complex form micelle-like clusters. On the other hand, analyses of small $Q$ portions of SANS distributions clearly showed that the arrangement of micelle-like clusters resembles a fractal packing of spheres. We showed that a protein/SDS complex can be characterized by four parameters extracted from the scattering experiment, namely, the average micelle size and its aggregation number, the fractal dimension characterizing the conformation of the micellar chains, the correlation length giving the extent of the unfolded polypeptide chains, and the numbers of micelle-like clusters in the complex.

## INTRODUCTION

It has been well known[1] that anionic surfactant sodium dodecylsulfate (SDS) is one of the most potent denaturant of water-soluble proteins. Since hydrophobic effects are the major driving force for the folding of water-soluble proteins into their native forms,[2] it is generally agreed in the literature[3,4] that the unfolding of proteins by SDS is caused by binding of SDS molecules to the hydrophobic portions of the polypeptide chain. However, there is no unanimity in the literature about the precise structure of the resultant protein/SDS complexes thus formed in aqueous solutions.[5] A similar problem of the interaction of SDS with water-soluble polymers and its resultant formation of polymer/SDS complexes has been important in industrial applications and the structure of such complexes has recently been elucidated.[6] Understanding of the structure of protein/detergent complexes is important even from practical point of view. It has been a common practice in protein biochemistry to determine molecular weights of proteins by performing electrophoresis of protein/SDS complexes in polyacrylamide gels, following the classic work of Weber and Osborn.[7] It appears that the precise understanding of the basic principle of SDS gel electrophoresis at the molecular level is still lacking.[8]

A well-known study of the structure of protein/SDS complexes by viscometry for a number of proteins by Reynolds and Tanford[3] concluded with a proposal of a prolate ellipsoidal model for the complexes with a high content of $\alpha$-helical structure. Size of the semiminor axis of the ellipsoid is constant for several proteins studied and is equal to approximately 18 Å, while that of the major axis is variable, proportional to the length of the polypeptide chain.

© 1990 John Wiley & Sons, Inc.
CCC 0006-3525/90/020335-12 $04.00
**Biopolymers**, Vol. 29, 335–346 (1990)

*Permanent address: Department of Biological Science and Biotechnology, Tsinghua University, Beijing, PROC.
†To whom correspondence should be addressed.

Recently a theoretical model for protein/SDS complexes was advanced by Lundahl et al.[9] They suggested that in a complex, SDS molecules form a flexible capped cylindrical micelle around which the hydrophilic segments of the polypeptide chain are helically wound. The bindings between polypeptide segments and the detergent molecules are mainly due to the hydrogen bonds. The hydrogen bond is between the nitrogen atom of the peptide bond and the sulfate oxygen of the detergent molecule.

In a lesser known study by Shirahama et al.,[10] the authors noticed that the free electrophoresis mobilities of the saturated polypeptide/SDS complexes were virtually constant, regardless of the molecular weight of the polypeptide, and that the mobility was compatible with that of the SDS micelle. They therefore proposed a model of the complexes called the "necklace" model, which assumed that the polypeptide chains are flexible in solution and micelle-like clusters of SDS are distributed along the unfolded polypeptide chains. In addition, the nmr study by Tsujip et al.[11] and by Oakes[12] confirmed that SDS molecules in the bovine serum albumin (BSA)/SDS complexes are in a micelle-like environment and clusters of surfactant molecules are formed on the protein, which supported the necklace model.

This picture of the protein/SDS complexes is consistent with the findings of a quasielastic light scattering study of complexes of bovine serum alblumin and ovalbumin (OVA) with SDS by Tanner, Herpigny, Chen, and Rha.[13] These authors observed that there were two diffusion constants associated with the complexes: one similar to that of a free SDS micelle, which did not change with SDS concentration and the other, a smaller diffusion constant, which presumably associated with that of the unfolded polypeptide chain, which became smaller with increased SDS concentration.

Recently Chen and Teixeira[14] undertook a small angle neutron scattering (SANS) study of BSA/lithium dodecylsulfate (LDS) complexes in a buffer solution near the pI value of BSA. These authors adapted the necklace model of Shirahama et al.[10] and developed a "fractal model" to account for the spatial correlation between the strings of micelles linked together by the unfolded polypeptide chains. The resultant neutron cross section calculated with the fractal model was in excellent agreement with SANS data, confirming the validity of the necklace model.

In this paper we extended the SANS measurement to two globular proteins—OVA (MW = 42,125) and BSA (MW = 66,114), and their complexes with SDS. By using the fractal model developed earlier, we were able to extract a set of parameters that characterize the structure and conformation of the protein/SDS complexes. We obtained the average micelle size and its aggregation number, the fractal dimension that characterizes the topological nature of the conformation of the unfolded polypeptide chains, the average numbers of micellar binding sites on a polypeptide chain, and the correlation length, which gives a measure of the extent of the unfolded chains.

## EXPERIMENTAL PROCEDURE

### Sample Preparation

Both BSA (Sigma, catalog no. A7517) and OVA (Sigma, catalog no. A7642) were protein standards used for SDS gel electrophoresis. SDS (BDH Chemicals) was of electrophoresis purity. All other chemicals used in this study were of analytical grade. $D_2O$ (99.8% purity) was used as the solvent for all samples. The amount of 0.1*M* acetate buffer (pD 5.5) with 0.5*M* NaCl was prepared. The pD chosen was close to the pI values of BSA (4.9) and OVA (4.9). The values of pD and ionic strength for the buffer solution were chosen so as to minimize the electrostatic interactions between proteins. A lower ionic strength buffer was also used. This was a 0.02*M* sodium phosphate buffer (pD 7.2) with 0.15*M* NaCl, a buffer similar to that used in routine SDS electrophoresis.

The protein and SDS stock solutions were first prepared with the $D_2O$ buffer. Protein concentration in the stock solution was 2% (g/dL) and that of SDS 6% (g/dL). Required protein/SDS solutions were then prepared by mixing suitable volumes of protein solutions, SDS solution, and buffer. At the same time, small amount of $\beta$-mercaptoethanol (Bio-Rad Laboratories) was added in order to disrupt the disulfide bonds. The concentration of $\beta$-mercaptoethanol in the protein/SDS solution was 0.5% (g/dL). We shall denote by 1/1, 1/1.5, 1/2, and 1/3, samples containing respectively, protein/SDS (w/w) = 1/1, 1/1.5, 1/2, and 1/3. After the mixing, the protein-SDS solutions were heated to 37°C until the solutions became clear and then kept at room temperature for 24 h.

### SANS Experiment

SANS measurements were made at the Low Angle Biology Spectrometer[15] located at the High Flux

Beam Reactor of the Brookhaven National Laboratory. Cold neutrons emerging from a 1.4 L liquid hydrogen moderator inside the reactor were first sent through a cold beryllium filter to remove short wavelength neutrons, and then further monochromated by reflection from a multilayer metallic mirror made by depositing alternate thin layers of nickel and titanium on a flat glass substrate. Quasi-monochromatic neutrons thus obtained have a mean wavelength of $\lambda = 4.5$ Å with wavelength spread $\Delta\lambda/\lambda = 0.08$. Neutrons scattered from the sample were detected by a 50 × 50 cm two-dimensional multidetector situated at a sample-to-detector distance of 144 cm. The detector consists of a matrix of 128 × 128 pixels with the individual pixel size of 0.39 × 0.39 cm. This configuration gives a Q range of 0.016 to 0.25 $Å^{-1}$ at a Q resolution $\Delta Q/Q \simeq 0.05$. The magnitude of the scattering vector **Q** is defined as $Q = (4\pi/\lambda)\sin(\theta/2)$ where $\theta$ is the scattering angle. Some measurements were made at PACE Small Angle Diffractometer located at the Orphee reactor in Saclay, France. Two wavelengths $\lambda = 5$ and 8 Å were used.

The solution samples were contained in flat disk-shaped quartz cells of window thickness 1 mm and path length 2 mm. Multiple samples were mounted on an automatic rotating sample changer maintained at a temperature of $T = 25.0 \pm 0.1$°C by circulating water from a constant temperature bath. Each measurement was of duration varying between 1/2 to 1 h.

Two-dimensional raw detector counts were first corrected for the room and electronics background and the empty cell scattering, and then normalized to a unit monitor counts. We denote the resultant intensity at pixel $(i, j)$ by $I^s_{ij}$. We then construct a normalized intensity by $N^s_{ij} = I^s_{ij}/(T_s t_s)$ where $T_s$ and $t_s$ are, respectively, the transmission and the thickness of the sample. In order to further correct for the nonuniformity of the pixel efficiency and to put the intensity finally into an absolute scale, we divide $N_{ij}$ by the scattering from a standard sample processed in the same way. The criterion of the standard sample should be that it is an isotropic scatter with a well-known cross section and it should be thin enough to avoid multiple scattering. In practice, 1 mm water ($H_2O$) sample at the room temperature approximately satisfies this criterion owing to its large known incoherent cross section of hydrogen atoms. A water sample, 1 mm in thickness, however, gives rise to an appreciable amount of multiple scattering that the signal needs to be corrected for the effect of multiple scattering by an empirical factor $f$. We thus performed a separate water sample calibration run to obtain $N^w_{ij} = I^w_{ij}/(T_w t_w)$ in an obvious notation. A two-dimensional data set of a ratio, $R_{ij} \equiv N^s_{ij}/N^w_{ij}$, was thus constructed. This two-dimensional data set $R_{ij}$ was then radially averaged to obtain a one-dimensional data set $R(Q_j)$. An absolute intensity $I(Q_i)$ in units of $cm^{-1}$, signifying the differential scattering cross section per unit volume of the sample, was finally calculated by the formula[16,17]

$$I(Q_i) = R(Q_i)\left(\frac{1 - T_w}{4\pi t_w T_w}\right) f \qquad (1)$$

where $T_w$ is the transmission factor of the water sample, $t_w = 0.1$ cm its thickness, and $f \simeq 1.37$ the multiple scattering correction factor for the wavelength $\lambda = 4.5$ Å.

## Neutron Cross Section

In general the scattering cross section for unit volume of sample, denoted by $I(Q)$, for a collection of identical particles in solution can be written schematically as[18]

$I(Q)$ = (no. of particle per unit volume) × (contrast factor between the particle and the solvent)$^2$ × (volume of the particle)$^2$ × (shape factor of the particle) × (interparticle structure factor accounting for the interference of scattered wave from different particles)

We shall give an analytical expression of the shape factor, which we also call the "particle structure factor," and the interparticle structure factor in next section. Here we merely wish to comment on an assumption we have made in this article. We assume the contrast factor to be dominated by the difference in scattering length densities between the hydrocarbons of the micellar core and the $D_2O$ solvent. We shall neglect the contrast between the polypeptide chain and the solvent in comparison. Our estimate was that the former is at least three times larger. Furthermore, we expect that the scattering intensity distribution due to the polypeptide chains to spread over different $Q$ ranges (smaller) from that of the micellar aggregates. In effect, we assume the unfolded proteins are invisible as compared to the micelles which form within their backbones.

## THEORETICAL MODEL

It was found in two previous experiments on protein/detergent interaction[10,14] that the data can be explained reasonably well by the so-called necklace model. This model assumed for the protein/SDS complex a structure consisting of a string of micelle-like clusters randomly distributed along the unfolded polypeptide chain and suspended in random orientations in solution. Suppose all the micelle-like clusters can be regarded as a uniform ellipsoid of revolution. One can then derive a theoretical cross section formulae for the analysis of SANS data. This is the fractal model.

The scattering intensity distribution for a collection of uniform ellipsoidal micelles in the necklace model can be written generally as

$$I(Q) = N_1\bar{N}(b_m - V_m\rho_s)^2\tilde{P}(Q)S(Q) \qquad (2)$$

where $N_1$ is the number density of the total surfactant molecules in solution, $\bar{N}$ the average aggregation number of micelle-like clusters, $b_m$ the scattering length of the surfactant molecule, $V_m$ its volume, and $\rho_s$ the scattering length density of $D_2O$ solvent. $\tilde{P}(Q)$ denotes the normalized particle structure factor of an ellipsoid, and can be written[17,18] as

$$P(Q) = \int_0^1 d\mu \left| \frac{3j_1(u)}{u} \right|^2 \qquad (3)$$

where $j_1(x) = x^{-2}\sin(x) - x^{-1}\cos(x)$, is the first-order spherical Bessel function. The variable $u$ is a function of the semimajor and semiminor axis of the prolate spheroid $a$ and $b$, and $\mu$ is the direction cosine between the symmetry axis of the spheroid and the **Q** vector, namely,

$$u = Qb\left[(a/b)^2\mu^2 + (1 - \mu^2)\right]^{1/2} \qquad (4)$$

The integration over $\mu$ in Eq. (3) essentially performs the orientational average of the ellipsoid with respect to the **Q** vector.

The $S(Q)$ function is the interparticle structure factor that takes into account the intermicellar positional correlations. $S(Q)$ can be defined, in general, in terms of the micellar pair correlation function $g(r)$ by[19]

$$S(Q) = 1 + n\int_0^\infty \mathrm{d}r\, 4\pi r^2 \frac{\sin Qr}{Qr} g(r) \qquad (5)$$

where $n$ is the number density of micelles in solution. We can simply derive the asymptotic behavior of $S(Q)$ at small $Q$ by the following argument: In a $D$ dimensional space, the number $N(r)$ of individual scatters within a sphere of radius $r$ is given by $N(r) = (r/R)^D$. The physical meaning of $D$ can be seen easily as a fractal dimension of the packing of the micellar clusters. For example, $D = 3$ means that the spheres are in a compact arrangement similar to three-dimensional packing of molecules in liquids. But in general $D$ can be a fractional number less than three for packings with open structures. The derivative of the above equation can be related to the asymptotic form of the pair-correlation function $g(r)$. From the definition of $g(r)$ one can derive a relation[14]

$$g(r) = \frac{D}{4\pi n}\frac{1}{R^D} r^{D-3} \qquad (6)$$

In addition, for the necklace model of the protein/detergent complexes, one expects that the correlation among micelles has a limited range. Therefore we assume the micelle–micelle correlation to have a finite range $\xi$, which is a measure of the extent of the unfolded polypeptide chain. Thus, we introduce a cutoff factor $\exp(-r/\xi)$ into Eq. (6), following an idea of Sinha et al.,[20] to get

$$g(r) = \frac{D}{4\pi n}\frac{1}{R^D} r^{D-3}\exp(-r/\xi) \qquad (7)$$

Upon substitution of Eq. (7) into Eq. (5) and taking the Fourier transform, we get

$$S(Q) = 1 + \frac{1}{(QR)^D}\frac{D\Gamma(D-1)}{\left[1 + (Q\xi)^{-2}\right]\left[(D-1)/2\right]} \times \sin\left[(D-1)\tan^{-1}(Q\xi)\right] \qquad (8)$$

where $R$ is an equivalent micellar radius, $R = (ab^2)^{1/3}$, for the ellipsoidal micelle, $D$ the fractal dimension of the micellar distribution in space, and $\xi$ the correlation length. A special case of Eq. (8) is when $D = 2$; it simplifies to

$$S(Q) = 1 + 2\left(\frac{\xi}{R}\right)^2 \frac{1}{1 + Q^2\xi^2} \qquad (9)$$

which is just the Ornstein–Zernike form of the

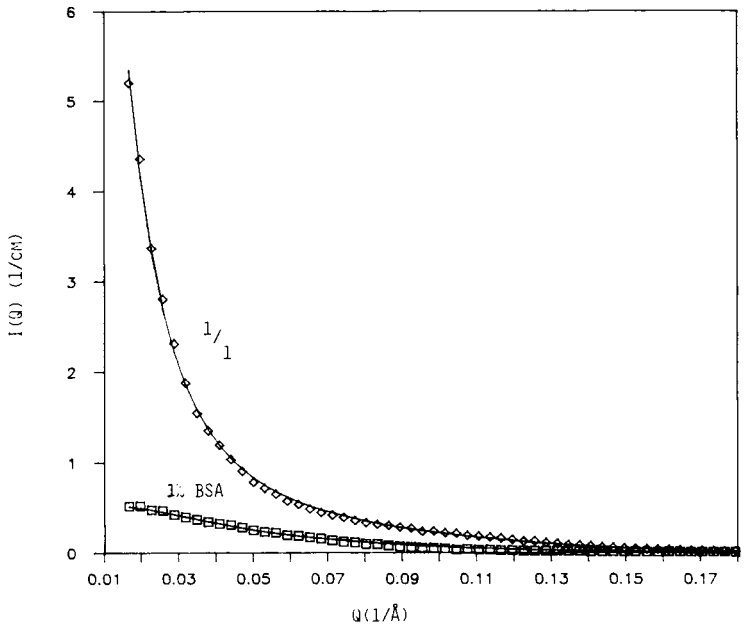


**Figure 1.** Absolute scattering intensity $I(Q)$ of 1% native BSA in buffer solution and of the 1/1 sample, plotted vs $Q$. Symbols are the experimental points for pure BSA (square) and for sample 1/1 (triangle). Solid lines are the best theoretical fits.

structure factor familiar in critical scattering from fluid.[21] One notable feature of Eq. (8) is that when $Q\xi \ll 1$, the structure factor approaches the limiting value

$$\lim_{Q\to 0} S(Q) = 1 + \Gamma(D+1)\left(\frac{\xi}{R}\right)^D \qquad (10)$$

In Eqs. (8) and (10), $\Gamma(x)$ denotes the gamma function. Since the micelle size $R$ is more or less fixed by the surfactant tail length, as the protein unfolds, $\xi$ increases and hence the value of $S(Q \to 0)$ increases sharply. In the opposite limit when $QR \gg 1$, $S(Q)$ approaches unity. In the intermediate $Q$ range ($1/\xi < Q < 2/R$), the structure factor has the form $S(Q) \sim (QR)^{-D}$, which is a general feature of the scattering from a fractal object.

## DATA ANALYSIS

In the previous section we derived a formula for the calculation of neutron cross section. We shall apply it in analyzing the experimental data in this section and to verify that the model is valid for the characterization of the protein/detergent complexes.

In Eq. (2) the unknown parameters are $D$, $\xi$, $N$, $a$, and $b$. Considering $\overline{N} = N_1/(N_pN)$, where $N_p$ is the number density of protein molecules in solution and $N$ is the number of micelles on a chain, we substitute $\overline{N}$ and rewrite Eq. (2) as

$$I(Q)(\mathrm{cm}^{-1}) = \frac{N_1^2}{N_pN}(b_m - V_m\rho_s)^2\tilde{P}(Q)S(Q) \qquad (11)$$

In this form, the unknown parameters are $D$, $\xi$, $N$, $a$, and $b$. Therefore, the independent parameters used in data fitting are $\xi$, $D$, $N$, $a$, and $b$.

In addition, SANS data for pure proteins in buffer solution were fitted to an ellipsoidal model without considering the protein/protein interaction.[17] This is sufficient for dilute protein solutions. The fitted parameters are $a = 71$ and $b = 19$ Å for BSA, and $a = 52$ and $b = 15$ Å for OVA.

Since there are five unknown parameters in the formula, it is impossible to extract them by a fitting program simultaneously. So the fitting procedure should be carried out in steps. The procedure we adopted is as follows: (1) From the experiment data in the large $Q$ range and the known surfactant tail length, we can determine $a$, $b$, and an approximate $N$. (2) We then fix $a$, $b$, and $N$ to fit the data in the entire $Q$ range using two other parameters, $D$ and $\xi$. According to the result obtained, we modify $a$, $b$, and $N$ slightly, if necessary, to make the fit better. (3) By systematic

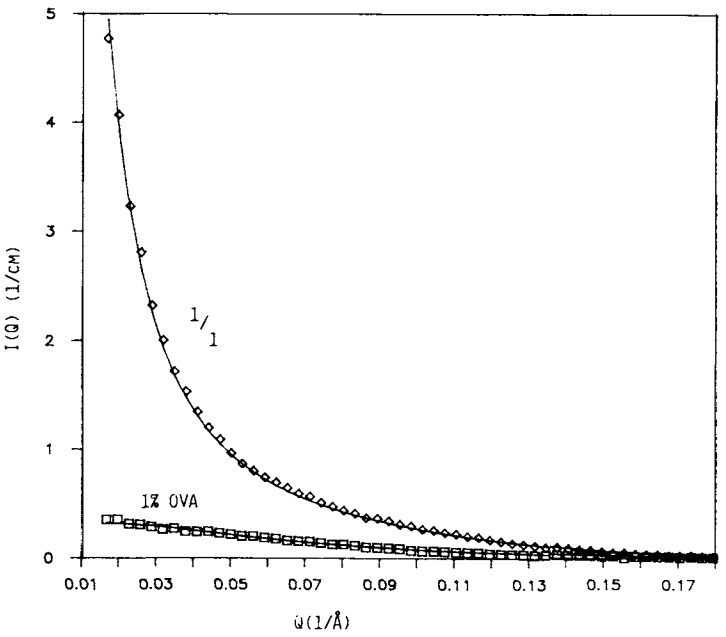


**Figure 2.** Absolute scattering intensity $I(Q)$ of 1% native OVA in buffer solution and of the 1/1 sample, plotted vs $Q$. Symbols are the experimental points for pure OVA (square), and for sample 1/1 (triangle). Solid lines are the best theoretical fits.

fitting of all data, we finally fix values of $a$, $b$, and $N$ to extract the remaining $D$ and $\xi$. Once these independent parameters are determined, other quantities, such as $\bar{N}$, the average SDS molecules per micelle-like cluster, can be calculated.

## RESULTS AND DISCUSSION

In order to illustrate the dramatic change in SANS intensity distribution from proteins to protein/detergent complexes, we compare, in Figs. 1 and 2, SANS intensity distributions of 1/1 samples with 1% pure protein solutions for BSA and OVA, respectively. It is clear from the figures that both the size and the number of the scattering unit in the 1/1 samples are markedly different from the 1% protein solutions since $I(Q \rightarrow 0)$ is proportional to the number and molecular weight of the scattering units. We also find no evidence for the intermicellar correlations of the three-dimensional short-range type, characteristic of a liquid-like system, since the scattered intensity distributions do not show an interaction peak at around 0.05 $Å^{-1}$.[22] Absence of the interaction peak confirms that micelles are not freely suspended in solutions. This is certainly the case, for the 1/1 samples, since the detergent concentration is below the saturation binding level. In fact, an ultracentrifugal photograph method[23] showed that the maximum bindings of SDS to BSA and OVA (disulfide bond intact), at 0.4$M$ ionic strength, to be 1.9 and 2.6 g (g SDS/g protein) respectively. In Figures 1–7 all the scattering data (symbols) are presented in an absolute intensity unit ($cm^{-1}$) as defined in Eq. (1). The theoretical curves (solid lines) were calculated by using Eq. (11). Sometimes, in order to separate different curves in a plot, for visual clarity, factors 5, 25, and 125 are multiplied to the absolute intensity distributions for samples 1/1.5, 1/2, and 1/3, as were done in Fig. 3, Fig. 4, Fig. 5 and Fig. 7.

### BSA / SDS Complex ($I$ = 0.6$M$)

BSA[24] is a transport protein that has the ability to bind hydrophobic ligands such as fatty acids. It has 17 disulfide bonds and 68% helix content, which indicates that $\alpha$-helices are the major structural components. It has been suggested[24] that BSA has three domains consisting of six paired subdomains. This implies that there are six high-affinity binding sites for fatty acids and each subdomain contains a hydrophobic face and a polar face.

Figure 3 shows a set of four intensity distributions measured in Saclay (France). These are samples with BSA/SDS wt ratios 1/1.0, 1/1.5, 1/2.0, and 1/3.0. We present them in log $I(Q)$ vs log $Q$ plots. Figure 4 shows another set of four intensity

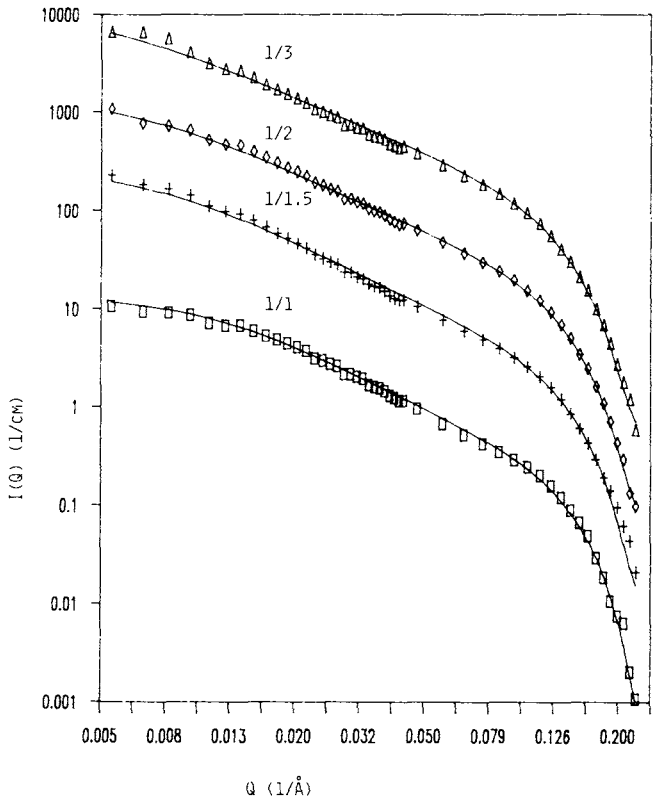


**Figure 3.** Absolute scattering intensity $I(Q)$, measured in Saclay, for the four samples studied (BSA/SDS, $I = 0.6M$), vs $Q$ in a log–log plot. Symbols are the experimental points for samples 1/1 (square), 1/1.5 (cross), 1/2 (diamond), and 1/3 (triangle). Solid lines are the best theoretical fits.

distributions measured in BNL (USA), for samples prepared in the same way as in Fig. 3. Both figures show that the theoretical calculations (solid lines) are in good agreement with the experimental data (symbols) over the entire $Q$ range for all samples. The parameters extracted are given in Tables I and II. We can see that the two sets of parameters extracted from two completely independent experiments are very close. Although the smallest $Q$ value we were able to access in BNL was only about 0.016 $Å^{-1}$, the result of fittings still give similar parameters as those from Saclay, and the latter set of data includes an additional $Q$ range, $Q < 0.016$ $Å^{-1}$. Therefore, we may trust the data for OVA, which were taken only at BNL, with a narrow $Q$ range.

For a sufficiently large $Q$ data (i.e., $Q > 0.1$ $Å^{-1}$), $S(Q) \to 1$, and the shape of $I(Q)$ depends only on $P(Q)$. The parameters contained in the $P(Q)$ function, such as $a$ and $b$, are thus more sensitive to this portion of data. In Figs. 3 and 4 we show that data in this portion of $Q$ are well fitted by assuming an ellipsoidal micelle. Thus, the assumption that SDS molecules aggregate into micelle-like clusters are well established. In a $Q$ range between 0.01 and 0.1 $Å^{-1}$, the fractal nature of micellar packing can be seen easily by plotting $\log I(Q)$ vs $\log Q$. For fractal aggregates we have $\log I(Q) \sim D \log Q$ in the intermediate $Q$ range ($1/\xi < Q < 2/R$). The slope of the straight line is thus related to the value of the fractal dimension $D$ and the magnitude of $I(Q)$ is sensitive to $\xi$.

Tables I and II show that $D$ decreases from about 2.1 to 1.65 and $\xi$ increases from 82 to 210 Å successively, with an increase of SDS concentration. This is consistent with an intuitive picture that the conformation of SDS/BSA complexes transforms gradualy from a compact globule to a more open random coil conformation as the denaturation proceeds. The $\xi$ value for 1/3 complex is consistent with the rms end-to-end distance of BSA in $6M$ GuHCL,[1] in which proteins are believed to have a random coil conformation. This shows that the $\xi$ is correlated with the extent of the unfolding

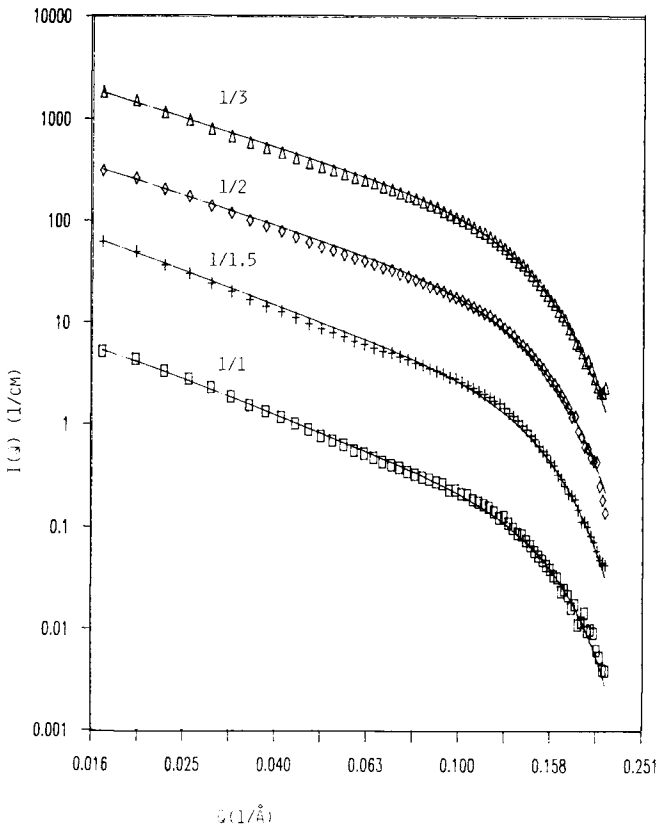


**Figure 4.** Absolute scattering intensity $I(Q)$, measured in BNL, for the four samples studied (BSA/SDS, $I = 0.6M$), vs $Q$ in a log–log plot. Symbols are the experimental points for samples 1/1 (square), 1/1.5 (cross), 1/2 (diamond), and 1/3 (triangle). Solid lines are the best theoretical fits.

of the polypeptide chain. Moreover, $N$, the numbers of micelle in a complex, increases during this process. This can be interpreted as a result of a further unfolding of the polypeptide chain. Interestingly, the $N$ ($N = 8$) we extracted from the 1/1 sample is compatible with the number of high affinity binding sites of a BSA molecule (= 6). The calculated micelle aggregation number $\bar{N}$ generally vary from 30 to 45, smaller than ordinary SDS micelles in water. To our knowledge, this is the first time that this information has been reported. However, a similar result was reported from a study of synthetic polymer/SDS complexes.[6] The reason of smaller $\bar{N}$ for the micelle-like clusters in protein/SDS complexes is unknown. One may conjecture that the side chains of amino acid residues probably have a strong effect on micellization. Then, one possible explanation would be that the hydrophobic portion of the polypeptide chain behaves like a nucleus of micellization to stabilize effectively the micelle-like cluster having a small aggregation number.

## OVA / SDS Complex ($I = 0.6M$)

OVA[25] is a monomeric protein. The protein consists of a single polypeptide chain, restrained probably by only one disulfide bond. A striking aspect of the amino acid composition of OVA is the fact that about 50% of its residues have hydrophobic nature. The helix content of OVA was estimated to be between 22 and 34%.

Figure 5 shows four intensity distributions measured in BNL, for the samples with OVA/SDS wt ratio 1/1, 1/1.5, 1/2, and 1/3. This figure shows that the theoretical calculations are in good agreement with the experimental data over the entire $Q$ range, for all samples. The parameters extracted are given in Table III. It is found that $D$ decreases from about 1.90 to 1.57 and $\xi$ increases from 101 to 188 Å successively with increasing SDS concentration. The $\xi$ value for 1/3 complex is consistent with the rms end-to-end distance of OVA in $6M$ GuHCL.[1] $N$ increases during this process too. A discussion similar to BSA/SDS can be made, ex-

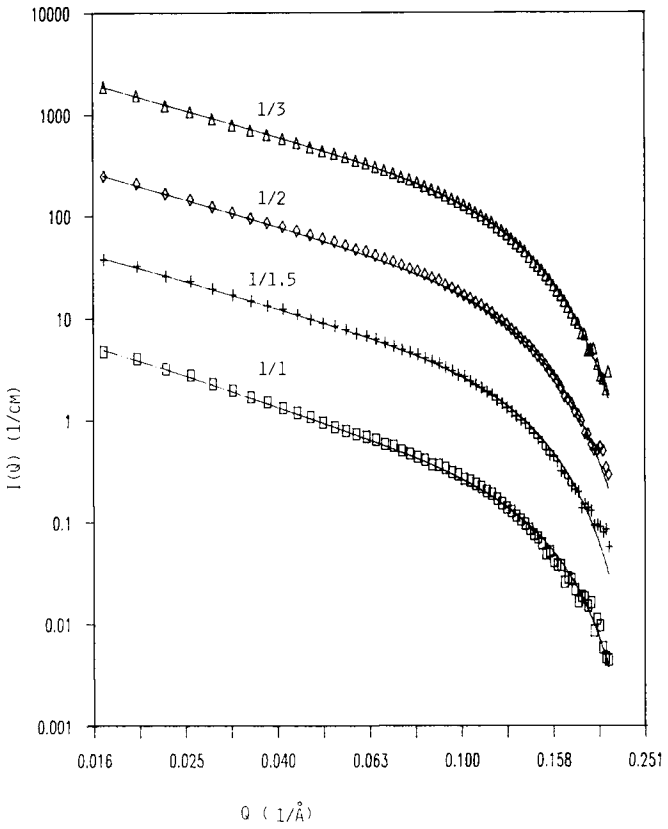


**Figure 5.** Absolute scattering intensity $I(Q)$, measured in BNL, for the four samples studied (OVA/SDS, $I = 0.6M$), vs $Q$ in a log–log plot. Symbols are the experimental points for samples 1/1 (square), 1/1.5 (cross), 1/2 (diamond), and 1/3 (triangle). Solid lines are the best theoretical fits.

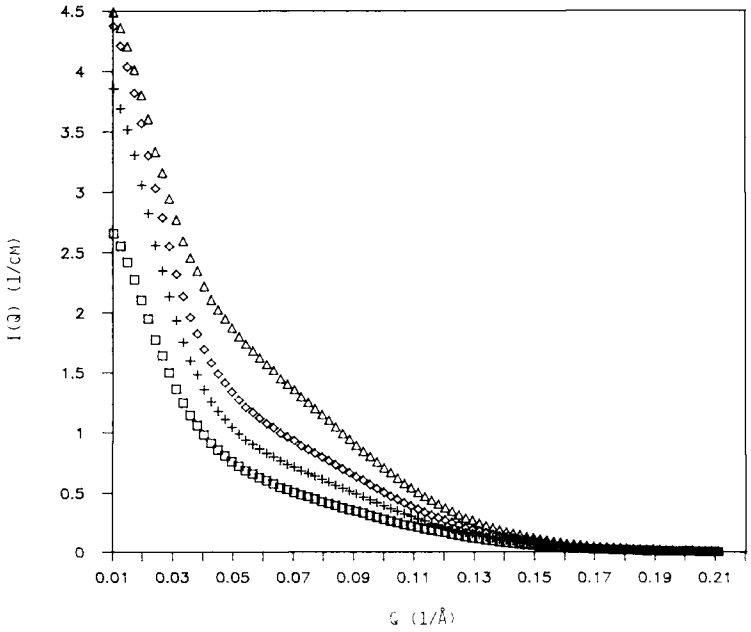


**Figure 6.** Absolute scattering intensity $I(Q)$, measured in BNL, for the four low ionic strength samples (BSA/SDS, $I = 0.2M$), plotted vs $Q$. Symbols are the experimental points for samples 1/1 (square), 1/1.5 (cross), 1/2 (diamond), and 1/3 (triangle).

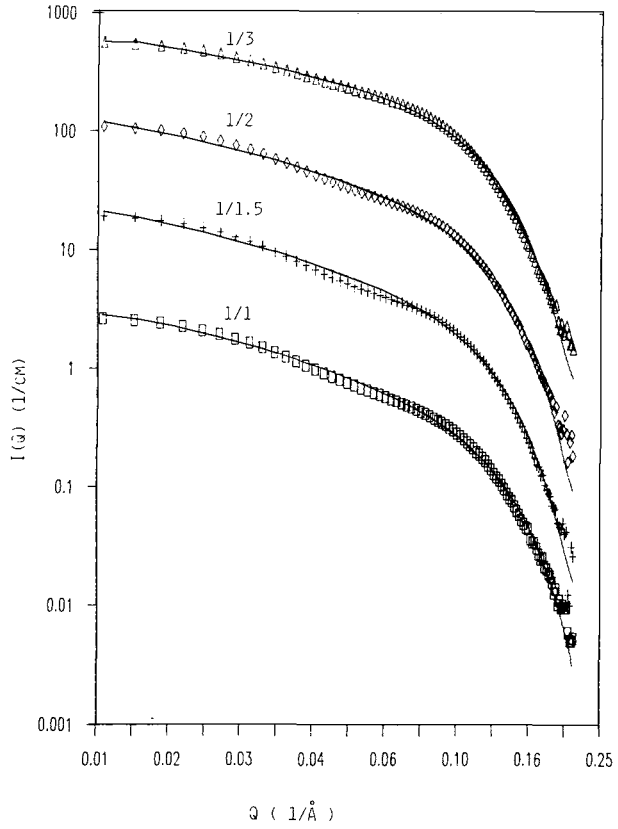


**Figure 7.** Absolute scattering intensity, measured in BNL, for the four low ionic strength samples (BSA/SDS, $I = 0.2M$), vs $Q$ in a log–log plot. Symbols are the experimental points for samples 1/1 (square), 1/1.5 (cross), 1/2 (diamond), and 1/3 (triangle). Solid lines are the best theoretical fits.

**Table I** Saclay Data ($I = 0.6M$)[a]

| BSA/SDS | $D$ | $\xi$ | $a$ | $b$ | $N$ | AGG |
|---|---|---|---|---|---|---|
| 1/1 | 2.00 | 82 | 23 | 18 | 8 | 29 |
| 1/1.5 | 1.90 | 127 | 25 | 18 | 8 | 43 |
| 1/2 | 1.75 | 152 | 26 | 18 | 11 | 42 |
| 1/3 | 1.65 | 208 | 27 | 18 | 18 | 39 |

[a]Unit for $\xi$, $a$, and $b$ is Å in all tables. $D$ = fractal dimension, $\xi$ = correlation length, $a$ and $b$ = semimajor and semiminor axes of an ellipsoid, $N$ = numbers of micelle-like clusters in a protein/SDS complex, AGG = $\bar{N}$ = mean aggregation number of micelle-like cluster.

**Table II** BNL Data ($I = 0.6M$)

| BSA/SDS | $D$ | $\xi$ | $a$ | $b$ | $N$ | AGG |
|---|---|---|---|---|---|---|
| 1/1 | 2.15 | 82 | 23 | 18 | 8 | 29 |
| 1/1.5 | 2.00 | 120 | 25 | 18 | 8 | 43 |
| 1/2 | 1.75 | 155 | 26 | 18 | 11 | 42 |
| 1/3 | 1.66 | 211 | 26 | 18 | 18 | 39 |

cept that a different molecular weight of OVA results in a different $N$. Comparing Table III with Tables II and I, we see that the value of $\bar{N}$, $a$, and $b$ are nearly identical. But a significant finding is that $D$ values of OVA/SDS complex are smaller than that of BSA/SDS complexes, and the $\xi$ of OVA/SDS complexes are comparable with or larger than that of BSA/SDS complexes. This is quite consistent with our expectation. Since OVA has 50% hydrophobic amino acid residues and low helix content, it is very likely that OVA/SDS complexes have a more expanded structure than BSA/SDS complexes. This is confirmed by comparing the values of $D$ and $\xi$ to that of BSA. In this sense $D$ and $\xi$ give significant information on the denaturation of proteins. Furthermore, $\xi$ can be used to estimate an average spacing $L$ between two neighboring micelles by the following argument: Suppose the structure of the 1/3 sample corresponds to an unperturbed chain along which micelle-like clusters are distributed; then $\xi \simeq \langle R^2 \rangle^{1/2} = N^{1/2}L$ holds. We therefore obtain $L_{\mathrm{OVA}} = 60$ Å and $L_{\mathrm{BSA}} = 50$ Å.

**Table III** BNL Data ($I = 0.6M$)

| OVA/SDS | $D$ | $\xi$ | $a$ | $b$ | $N$ | AGG |
|---|---|---|---|---|---|---|
| 1/1 | 1.90 | 101 | 22 | 18 | 5 | 29 |
| 1/1.5 | 1.68 | 123 | 23 | 18.2 | 5 | 44 |
| 1/2 | 1.61 | 172 | 25 | 18 | 7 | 42 |
| 1/3 | 1.57 | 188 | 25 | 18 | 10 | 44 |

### BSA / SDS Complex ($I = 0.2M$)

The buffer condition for these samples was prepared in a way similar to the routine SDS gel electrophoresis. Figure 6 shows four experimental intensity distributions, corresponding to the samples with BSA/SDS wt ratio 1/1, 1/1.5, 1/2, and 1/3 at $0.2M$ ionic strength. It is a linear plot of $I(Q)$ vs $Q$. We see that the absolute intensity of the 1/1 sample is considerably smaller than that shown in Figs. 1 and 2 in the small $Q$ region. Furthermore, we see from Fig. 6 that as $Q$ becomes smaller, the increase of $I(Q)$ for 1/3 sample is obviously slowed. This indicates that the binding is saturated as the SDS/protein wt ratio approaches 3 at $I = 0.2M$, and a certain amount of free micelles may be formed in the case of 1/3 samples. Since this phenomenon is not observed for the case of $I = 0.6M$, our result is consistent with the fact that increasing ionic strength can increase the max-

imum SDS binding level.[23] On the other hand, since the pD value chosen here was 7.2, BSA and OVA carry more negative charges. The maximum binding level would therefore decrease due to the repulsion between negative charges of proteins and SDS head groups. The comparison of theoretical calculations and experimental data are made in log $I(Q)$ vs log $Q$ plots in Fig. 7. The fitted parameters are listed in Table IV. Figure 7 shows that the fitting for $Q > 0.1$ Å$^{-1}$ is still very good. This means that SDS molecules still form micelle-like clusters in the complexes as in $I = 0.6M$. But the values of $\bar{N}$, $a$, and $b$ are slightly larger than those given in Tables I, II, and III. The fits for $Q <$ 0.1 Å$^{-1}$ are not satisfactory. Compared with the corresponding parameters for the $I = 0.6M$ case, both $\xi$ and $D$ are smaller. The smaller $\xi$ can be explained by the compression of the random coils due to repulsion between different complexes, but it seems that $D$'s in the present case have no significant meaning. Further work is necessary to elucidate the ionic strength and pH dependencies of the structure of protein/detergent complexes.

**Table IV** BNL Data ($I = 0.2M$)

| BSA/SDS | $D$ | $\xi$ | $a$ | $b$ | $N$ | AGG |
|---|---|---|---|---|---|---|
| 1/1 | 1.44 | 71 | 24.5 | 18 | 6 | 38 |
| 1/1.5 | 1.27 | 101 | 27 | 18.8 | 8 | 43 |
| 1/2 | 1.17 | 120 | 27 | 19 | 11 | 42 |
| 1/3 | 1.05 | 156 | 28 | 19 | 14 | 50 |

## CONCLUSION

In summary, our analyses of the absolute intensities of SANS data established the following picture of the protein/SDS complexes in high ionic strength solution ($I = 0.6M$):

1. SDS molecules in protein/SDS complexes form micelle-like clusters, each of which can be approximated as an ellipsoid micelle.

2. The packing of the micelle-like clusters in a protein/SDS complex has a fractal-like feature having two characteristic parameters: a fractal dimension $D$ and a correlation length $\xi$.

3. $D$ and $\xi$ can be used to characterize the conformation of denaturated proteins.

4. The average number of micelle-like clusters per polypeptide chain $N$, the average aggregation number of the micellar cluster $\bar{N}$, and the dimensions of the micelle $a$ and $b$ can be determined.

5. The saturation binding supposedly occuring at SDS/protein wt ratio $\simeq 1.4$[3] is not a clear-cut transition. We believe that even after the binding ratio of 1.4 is reached, SDS molecules continue to bind or be absorbed into the partially unfolded polypeptide chain.

Based on the above results, a schematic two-dimensional picture is drawn in Fig. 8 to represent the structure of the protein/SDS complexes. The details of the local structure of the micelle-like cluster is not fully clear based only on these fitted parameters.

For the low ionic solutions ($I = 0.2M$) the necklace model is not completely satisfactory. An alter-

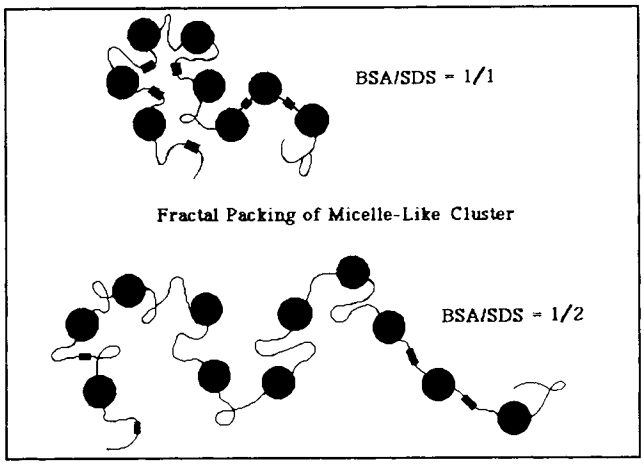


**Figure 8.** Schematic representation of a protein/SDS complex in aqueous solution. Black dots are micelle-like clusters and solid line the unfolded polypeptide chain. Small black cylinders represent the collapsed structure (e.g., $\alpha$-helix).

native model of Lundahl et al.[9] might be appropriate. Further SANS experiments for the low ionic strength cases are in progress.

We are grateful for Dr. D. Schneider for assistance in setting up SANS spectrometer at BNL. This research is supported by NSF grants administered through The Biotechnology Process Engineering Center and The Center for Materials Science and Engineering of MIT.

## REFERENCES

1. Tanford, C. (1968) *Adv. Protein Chem.* **23**, 121–282.
2. Kautzmann, W. (1959) *Adv. Protein Chem.* **14**, 1–63.
3. Reynolds, J. A. & Tanford, C. (1970) *Proc. Natl. Acad. Sci. USA* **66**, 1002–1007.
4. Tipping, E., Jones, M. N. & Skinner, H. A. (1974) *J. Chem. Soc. Faraday Trans. I* **70**, 1306–1315.
5. Makino, S. (1979) *Adv. Biophys.* **12**, 131–184.
6. Cabane, B. (1984) *J. Phys.* **43**, 1529–1542.
7. Weber, K. & Osborn, M. (1969) *J. Biol. Chem.* **241**, 4406–4412.
8. Cantor, C. R. & Schimmel, P. R. (1980) *Biophysical Chemistry*, Part 2, Freeman, San Francisco, CA.
9. Lundahl, P., Greijier, E., Sandberg, M., Cardell, S. & Eriksson, K.-O. (1986) *Biochim. Biophys. Acta* **873**, 20–26.
10. Shirahama, K., Jsujip, K. & Takagii, T. (1974) *J. Biochem.* (Tokyo) **75**, 309–318.
11. Tsujip, K. & Takagii, T. (1975) *J. Biochem.* **77**, 511–519.
12. Oakes, J. (1974) *J. Chem. Soc. Faraday Trans. I* **70**, 2200–2209.
13. Tanner, R. E., Herpigny, B., Chen, S. H. & Rha, C. K. (1982) *J. Chem. Phys.* **76**, 3866–3872.
14. Chen, S. H. & Teixeira, J. (1986) *Phys. Rev. Lett.* **57**, 2583–2586.
15. Schoenborn, B. P., Ramakrishnan, V. & Schneider, D. (1986) *Physica* **B137**, 214–220.
16. Jacrot, B. & Zaccai, G. (1981) *Biopolymers* **20**, 2413–2426.
17. Chen, S. H. & Lin, T. L. (1987) in *Methods of Experimental Physics* **23**, Part B, Price, D. L. and Sköld, K., Eds., Academic Press, New York.
18. Chen, S. H. (1986) *Ann. Rev. Phys. Chem.* **37**, 357–399.
19. Chen, S. H. (1972) in *Physical Chemistry*, Henderson, D., Ed., Academic Press, New York.
20. Sinha, S. K., Freltoft, T. & Kjems, J. (1984) in *Kinetics of Aggregation and Gelation*, Family, F. & Landau, D. P., Eds., Elsevier Press, Amsterdam.
21. Ornstein, L. S. & Zernike, F. (1914) *Proc. Natl. Acad. Sci. USA* **17**, 793.
22. Bendedouch, D., Chen, S. H. & Koehler, W. C. (1983) *J. Phys. Chem.* **87**, 2621–2628.
23. Nelson, C. A. (1971) *J. Biol. Chem.* **25**, 3895–3901.
24. Brown, J. R. & Shockley, P. (1978) in *Albumin: Structure, Biosynthesis, Function*. Peters, T. and Sjöholm, T., Eds., Pergamon Press, New York.
25. Taborsky, G. (1974) *Adv. Protein Chem.* **28**, 34–50.

*Received October 31, 1988*
*Accepted January 26, 1989*